Novel H_2-H_2O Clathrates at High Pressures

Willem L. Vos, Larry W. Finger, Russell J. Hemley, and Ho-kwang Mao

*Geophysical Laboratory and Center for High Pressure Research, Carnegie Institution of Washington,
5251 Broad Branch Road N.W., Washington, D.C. 20015*

High-pressure optical and x-ray studies of H_2-H_2O mixtures have revealed the formation of the first hydrogen clathrate hydrates. A rhombohedral hydrate with a H_2O sublattice similar to ice II and a H_2:H_2O ratio of 1:6 is stable between 0.75 and 3.1 GPa (295 K). Above 2.3 GPa, a novel hydrate forms with the H_2O molecules in a cubic diamond structure and with a very high H_2:H_2O stoichiometry of 1:1. The H_2 molecules occupy voids in the H_2O framework, thus improving the packing efficiency and stabilizing this hydrate to very high pressures of at least 30 GPa.

The properties of hydrogen and water at high pressures are of fundamental interest to condensed matter physics and chemistry as well as planetary astronomy [1–5]. Despite this importance, the behavior of mixtures of these components has remained unknown at pressures above 0.25 GPa [6]. Whereas mixtures of water and other molecules (such as Ar, Kr, Xe, N_2, CH_4, etc.) have a strong tendency to undergo phase separation in the fluid phase [6], they often form solid compounds at low temperature and ambient pressure called clathrate hydrates. These are hydrogen bonded networks of water molecules that form cages in which the other, guest, molecules are contained by van der Waals forces (see, e.g., [7]). The total amount of guest molecules relative to water is less than 1:5$\frac{2}{3}$ [7]. Two cubic clathrate structures have been known for a long time; they have water sublattices that differ from any of the known ice phases [8]. Because these frameworks have cages that are much larger than small molecules such as hydrogen, such hydrogen-water compounds have never been observed [7]. A recent neutron diffraction study at 0.5 GPa, however, revealed a rhombohedral helium clathrate with a novel H_2O structure related to ice II with much smaller cages [9]. It is therefore vital to investigate whether hydrogen forms similar small-cage clathrates at high pressures.

Clathrate hydrates are expected to break down at moderate pressures on the order of several GPa, because the compression of the pure gaseous guest species will outweigh the less effective packing of the clathrate phase in the free energy balance at higher pressure [7]. Indeed, a stability limit of 1.8 GPa was recently found in a cubic N_2 clathrate [10]. The ice-II type small-cage clathrate was only studied up to 0.5 GPa [9]. Therefore, it is important to assess the high-pressure stability limits of such a clathrate and investigate whether at higher pressure new types of clathrates occur.

In this Letter, we describe the formation of two new compounds (denoted C_1 and C_2) of hydrogen and water at high pressures. The H_2O sublattice of C_1 is similar to the ice phase II, thus closely resembling the small-cage helium clathrate [9]. At higher pressures, C_1 becomes unstable, and a novel type of clathrate, C_2, forms. The H_2O sublattice of C_2 has a diamondlike structure, similar to the ambient-pressure metastable ice phase I_c, whereas the hydrogen molecules occupy voids in the open H_2O frameworks, thus forming a stoichiometric compound with a very high H_2:H_2O stoichiometry close to 1:1 (see Fig. 1). Interestingly, the structure of the C_2 phase is also related to that of the high-ressure ice phase VII which is formed of two separate ice I_c-like hydrogen-bonded sublattices, that are interpenetrating but not cross linked [8]; the C_2 phase can be viewed as an ice VII structure in which one H_2O sublattice is completely replaced by H_2.

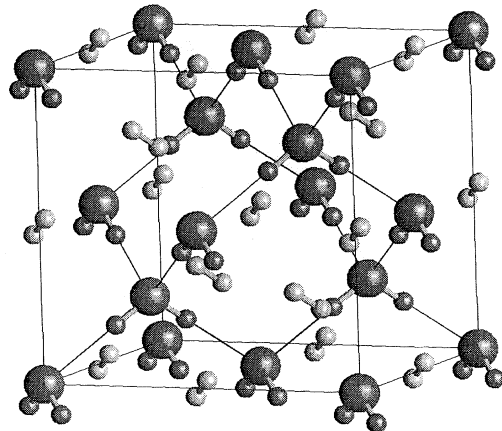Four separate experiments were performed in Mao-Bell diamond-anvil cells [11]. BeCu gaskets were used to

FIG. 1. Crystal structure of the new cubic clathrate (C_2 phase). The origin of $Fd\bar{3}m$ is set at the $4\bar{3}m$ site. The H_2 molecules are shown as light dumbbells in two orientations; however, due to their quantum nature they have an approximately spherical charge distribution. Similarly, the protons (small dark spheres) associated with H_2O are shown in ordered positions; however, x-ray data indicate they are disordered over two of the four possible positions that are tetrahedrally located ~ 1 Å from the oxygen ions (large dark spheres). The hydrogen bonds between different water molecules are indicated as thin dark lines.

0031-9007/93/71(19)/3150(4)$06.00

avoid reaction with H_2 [12]. The samples were loaded by filling the gasket hole with doubly distilled and de-ionized water and an air bubble. The cell was then placed in a gas loading vessel, in which the air in the bubble was purged and replaced by ultrapure (99.99%) H_2 gas at about 0.2 GPa pressure. The compositions were estimated from the visual appearance of the sizes of the two fluid phases at low pressure—identified by Raman spectroscopy and visual observations—and the known molar volumes of the pure components [13,14]. The accuracy of 5–10 mol% is mainly limited by the estimates of the sizes of the phases. Hereafter, we express compositions in mol% H_2. The sample compositions studied were 27%, 29%, 43%, < 48%, and 63%. The experiments were done with increasing load, because during decompressing the most volatile phase may preferentially leak out; after decompression of the 63% sample *less than* 48% H_2 was found [15]. Pressures were determined by the linear ruby fluorescence method [16]. The temperature correction to the ruby scale was taken from Ref. [17] and the accuracy of the pressure is estimated as 0.2 GPa. Temperatures were measured with thermocouples and are accurate to about 5 K. Raman spectroscopy was performed using various Ar^+ laser lines for excitation and a Dilor XY triple spectrometer equipped with an l-N_2 cooled charge coupled device detector. X-ray diffraction experiments

were done on the polychromatic synchrotron beam line X17C of NSLS, Brookhaven National Laboratory. Single crystal x-ray diffraction experiments were also performed using a four-circle diffractometer with monochromatic Mo $K\alpha$ radiation. All x-ray diffraction experiments were done at 295($\pm$ 3) K.

The results of a detailed study of the phase equilibrium in this system at 290–450 K and 0.7–3.2 GPa are shown in Fig. 2, along with the established phase diagram of H_2O [18]. The bold curves are three-phase lines involving a H_2O-rich fluid phase F_1, a H_2-rich fluid phase F_2, and three crystalline phases, C_1, C_2, and ice VII. Quadruple points are indicated by large circles. At 0.75 GPa and room temperature, microscopy revealed that birefringent C_1 is in equilibrium with F_1 and F_2. To investigate the structure of the C_1 phase, *in situ* polycrystalline x-ray diffraction measurements were performed at 1.6 and 2.1 GPa with the 63% sample. An example of a diffraction pattern at $2\theta = 8°$ is shown in Fig. 3. Several patterns at different scattering angles yielded a total of 24 diffraction lines that could be indexed to a hexagonal unit cell with $a = 12.736(2)$ Å and $c = 5.968(2)$ Å at 2.1 GPa. The reflections fulfill the condition $-h+k+l=3n$ (n is an integer) of rhombohedral structures (Fig. 3). Notably, this structure is distinct from that of the stable phase of pure H_2O in the same pressure range (ice VI), which is tetragonal with $a \sim 6.3$ Å and $c \sim 5.8$ Å [8]. A subsequent monochromatic x-ray experiment at 1.7 GPa on a single crystal that was carefully grown from the melt confirmed the rhombohedral space group $R\bar{3}$. Refinement with a structure containing 36 water molecules resulted in $R = 0.24$ and $R_w = 0.13$ [19,20]. The H_2O sublattice is similar to the structure of ice II, and it has six cages per unit cell [8]. Therefore, this new hydrogen
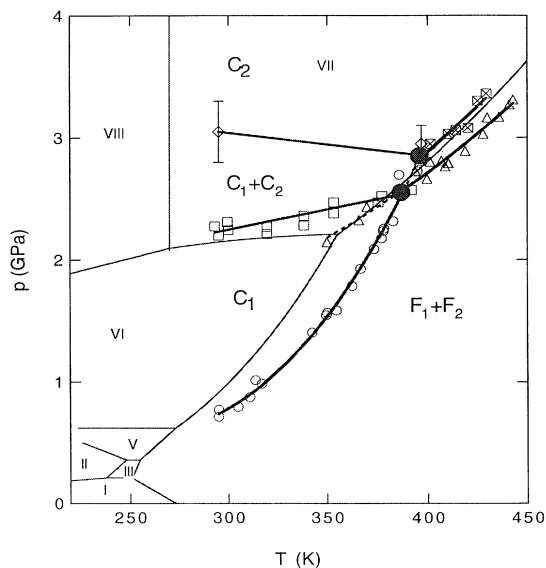

FIG. 2. *P-T* phase diagram of pure water (thin lines) and *P-T* projection of the phase diagram of hydrogen water (symbols and heavy lines). For pure water, only the stable phase lines have been taken from Ref. [8]. The open circles indicate the $F_1 + C_1 + F_2$ three-phase line, the open squares $C_1 + C_2 + F_2$, the triangles $F_1 + C_2 + F_2$, the diamonds VII + $C_1 + C_2$, and the crossed squares VII + $F_1 + C_2$. The large filled circles indicate the quadruple points $F_1 + C_1 + C_2 + F_2$ and VII + $F_1 + C_1 + C_2$. The metastable extension of the $F_1 + C_2 + F_2$ line has been observed below the quadruple point (dashed curve).
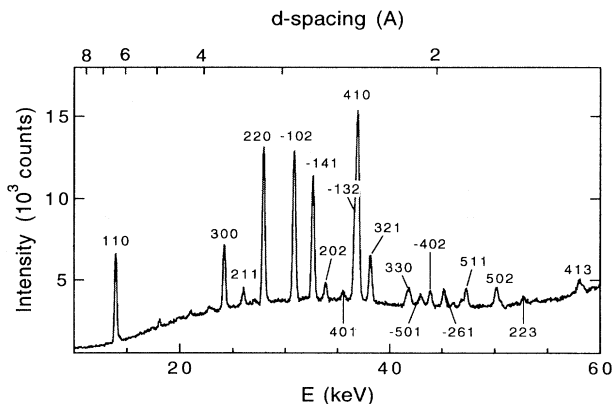

FIG. 3. Energy dispersive diffraction pattern of the C_1 phase at 2.1 GPa in the 63% sample at $2\theta = 7.990°$. The upper scale is calculated from the lower one using $Ed = 88.977$ keV Å. The diffraction lines are indicated by their indices. Other features are not associated with C_1, because they did not reproduce in patterns taken at $2\theta = 7.5°$, 10°, and 15°. Note that the crystal grains are large compared to the x-ray beam; therefore the intensities cannot be used for structure refinement.

clathrate has a structure similar to the small-cage helium clathrate observed by Londono, Kuhs, and Finney [9].

The Raman spectrum of the C_1 phase (Fig. 4) reveals sharp lattice translational modes (v_T), indicative of an ordered proton structure as in ice II [21]; however, the O-H stretch frequency of 3130 cm^{-1} is close to that of ice VI, which is surprising in view of the structural differences. The H_2 molecules were not observable with x-ray diffraction due to their low scattering cross section, but were clearly observed on the basis of a sharp H_2 vibron (Q_1) and two rotons $S_0(J)$ in the Raman spectrum. The vibron frequency is only 1 to 2 cm^{-1} higher than that of pure hydrogen [22]. The H_2 content of the solid phase was estimated to be between 10–20 mol% from the intensities of the vibron and roton bands, relative to those in the H_2-rich fluid phase when it was spatially well separated from the C_1 crystals. This is consistent with the structure described above, that corresponds to a H_2:H_2O molar ratio of 1:6.

At 2.3 GPa, visual observations of the 43% and 63% samples revealed that the solid phase C_1 and the fluid phase F_2 are in equilibrium with a new optically isotropic solid phase C_2 on the $C_1 + C_2 + F_2$ three-phase line (see Fig. 2). The two phases C_1 and C_2 coexist between 2.3 and 3.1 GPa because $H_2 + H_2O$ is a binary system. Polycrystalline x-ray diffraction of the 63% sample showed that the C_2 phase is cubic, with a lattice parameter $a = 6.434(1)$ Å at 3.1 GPa (see Table I), which is a little less than the equivalent lattice parameter of ice VII (2×3.330 Å) [2]. Similar experiments on the 29% sample revealed that C_2 is stable to at least 30 GPa. A monochromatic x-ray experiment at 2.8 GPa on a single

crystal that was carefully grown from the fluid phases showed systematic extinctions that are consistent with space group $Fd3m$. Refinement yielded a structure with eight water molecules arranged on a diamond structure (Fig. 1), as in ice I_c [8]. The unit cell volume of C_2 is much bigger than that of ice I_c extrapolated to the same pressure [8], indicating that there are additional hydrogen molecules in the structure. The locations of the H_2 molecules were found in different electron density maps due to the higher quality intensities than were obtained with the C_1 phase ($R = 0.054$ and $R_w = 0.034$) [20]. The molecules occupy the voids between the H_2O molecules that also form a diamond structure (Fig. 1).

The composition of the C_2 phase was estimated in two experiments. With the (43 ± 10) mol% H_2 sample, we observed only the C_2 phase and no evidence of phase separation between 2.3 and 6.8 GPa at room temperature; hence this represents the composition of C_2. Raman spectroscopy of the OH stretching modes with the < 48% sample revealed that the C_2 phase was in equilibrium with ice VII at pressures beyond 3 GPa at room temperature, indicating that the composition of C_2 is larger than the sample composition. Therefore we conclude that the H_2:H_2O stoichiometry is close to 1:1. The result is in agreement with the above structural assignment with all voids in the H_2O framework filled by H_2, as expected for a close-packed structure at high pressure.

Further information on the H_2 molecules in the C_2 phase was obtained from Raman measurements (Fig. 4). The vibron is on the order of 5–10 times more intense than in the C_1 phase, indicating that the C_2 phase is rich in hydrogen. The frequency is about 10 to 20 cm^{-1} higher than in pure H_2 [22], and increases with pressure. The linewidth of the vibron is narrower than the H_2-rich fluid phase, which is consistent with the centers of mass of the molecules being localized. The rotons are also very intense, significantly stronger than the lattice translational modes (v_T), and are very close to those observed for the fluid. This result indicates that J is still a good rotational quantum number for H_2 in the clathrate.

In Fig. 4, the Raman shift of the O-H stretch mode in the C_2 phase at 2.3 GPa is 3210 cm^{-1} which is clearly
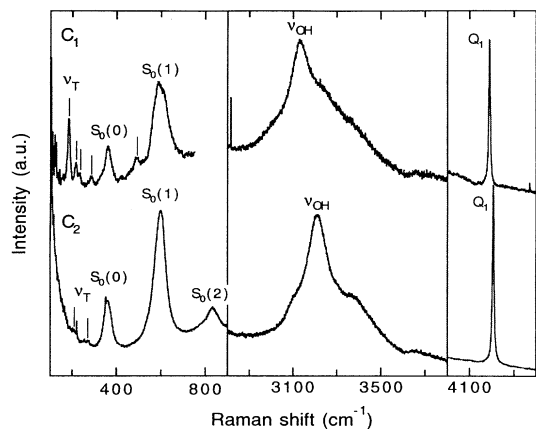
FIG. 4. Raman spectra of the C_1 phase (upper panels) and C_2 phase (lower panels) at 2.3 GPa. The upper and the lower central spectra were recorded in the 63% sample, and the remaining ones in the 43% sample. Translational lattice modes (v_T) are indicated with ticks, H_2 rotons by $S_0(J)$, the O-H stretching vibration by v_{OH}, and the H_2 stretching vibration by Q_1.

TABLE I. Observed and calculated d spacings of reflections for the cubic C_2 phase observed at 3.1 GPa. The lattice parameter is $a = 6.434(1)$ Å.

hkl	d obs. (Å)[a]	d calc. (Å)
111	3.712	3.714
220	2.273	2.274
311	1.940	1.939
400	1.608	1.608
331	1.476	1.476
422	1.313	1.313

[a]The uncertainty is approximately 0.1%.

smaller than the value of 3290 cm^{-1} of ice VII at the same pressure [23]. The reduced O-H frequency is the result of a reduced O-H $\cdots$ O distance: According to the x-ray diffraction measurements, the O-H $\cdots$ O distance is clearly smaller in the C_2 phase compared to ice VII (2.79 vs 2.89 Å) [8]. When the frequencies of the two phases are compared at the same O-H $\cdots$ O distance instead of the same pressure, however, they are identical.

Microscopy, Raman, and x-ray observations were used to determine the P-T phase diagram (see Fig. 2). Two invariant quadruple points, $F_1 + C_1 + C_2 + F_2$ at 387 K and 2.55 GPa and VII$+F_1 + C_1 + C_2$ at 396 K and 2.85 GPa, were located. The first point is defined at the intersection of three experimentally observed univariant curves: the melting curve of C_1 ($F_1 + C_1 + F_2$), the first appearance of C_2 ($C_1 + C_2 + F_2$), and the melting curve of C_2 ($F_1 + C_2 + F_2$). The second point is defined by two univariant curves: the breakdown curve of C_1 into ice VII and C_2 (VII$+C_1 + C_2$) and the eutectic curve of VII$+F_1 + C_2$. The two points are connected by the univariant curve $C_1 + C_2 + F_1$. The last univariant related to the two points, VII$+F_1 + C_1$, can only be measured with compositions smaller than C_1 (14 mol%) and has not been determined. For more details, see Ref. [18].

In conclusion, we have for the first time studied a molecular mixture containing water to high pressures in excess of 2 GPa and observed two new hydrogen hydrates C_1 and C_2. The discovery of C_1 and the result of Ref. [9] suggest that this structure is favorable for small molecules. The upper stability limit of 3.1 GPa agrees qualitatively with the prediction of Ref. [7] and it indicates that the cagelike structures have a stability range limited to moderate pressures. We have identified a clathrate transition sequence from C_1 to a new type, C_2, that is stable to ultrahigh pressures. It consists of two interpenetrating diamondlike sublattices, one for the H_2O host molecules and one for the H_2 guests. This structure can accommodate small guest molecules (or medium-size molecules becoming small at high compression) with a high packing efficiency, thus being a favorable structure at high pressures. It should be investigated whether other small molecules such as helium and neon show a similar transition sequence. Finally, because both C_1 and C_2 have higher melting temperatures than the pure ices at the same pressure (see Fig. 2), clathrates are expected to be of considerable importance to planetary interior layers of H_2-He and ices where high pressures and temperatures prevail.

[1] C. Lee et al., Phys. Rev. Lett. 69, 462 (1992).

[2] R. J. Hemley et al., Nature (London) 330, 737 (1987).

[3] A. Polian and M. Grimsditch, Phys. Rev. Lett. 52, 1312 (1984).

[4] H. K. Mao and R. J. Hemley, Am. Sci. 80, 234 (1992).

[5] I. F. Silvera, in Frontiers of High Pressure Research, edited by H. D. Hochheimer and R. D. Etters (Plenum, New York, 1991), p. 101.

[6] E. U. Franck, Physica (Amsterdam) 139 & 140B, 21 (1985).

[7] J. I. Lunine and D. J. Stevenson, Astrophys. J. Suppl. Ser. 58, 493 (1985).

[8] B. Kamb, in Physics and Chemistry of Ice, edited by E. Whalley, S. I. Jones, and L. W. Gold (Royal Society of Canada, Ottawa, 1973), p. 28.

[9] D. Londono, W. F. Kuhs, and J. L. Finney, Nature (London) 332, 141 (1988).

[10] M. G. E. van Hinsberg, M. I. M. Scheerboom, and J. A. Schouten, J. Chem. Phys. 99, 752 (1993).

[11] H. K. Mao and P. M. Bell, Carnegie Inst. Washington Yearbook 79, 409 (1989).

[12] J. A. Schouten, L. C. van den Bergh, and N. J. Trappeniers, Chem. Phys. Lett. 114, 401 (1985).

[13] R. L. Mills et al., J. Chem. Phys. 66, 3076 (1978).

[14] L. Haar, J. S. Gallagher, and G. S. Kell, NBS/NRC Steam Tables (Hemisphere Publishing, New York, 1984).

[15] A similar effect has been reported earlier in the system N_2-He; see W. L. Vos and J. A. Schouten [Physica (Amsterdam) 182A, 365 (1991)]. We can only place an upper bound on the composition of the sample after unloading, because the H_2-rich region did not fill up the full thickness of the sample space.

[16] G. Piermarini, S. Block, J. D. Barnett, and R. A. Forman, J. Appl. Phys. 46, 2774 (1975).

[17] W. L. Vos and J. A. Schouten, J. Appl. Phys. 69, 6744 (1991).

[18] W. L. Vos et al., in Proceedings of the Joint AIRAPT/APS Topical Conference on High Pressure Science and Technology, Colorado Springs, 1993, edited by S. Schmidt (American Institute of Physics, New York, to be published).

[19] The refinements were performed using RFINE90. See L. W. Finger and E. Prince, NBS Technical Note 854 (U.S. GPO, Washington, 1975).

[20] The R factor is defined as $R := \{\sum |[F_{obs}(hkl)| - |F_{calc}(hkl)|]\}/\sum |F_{obs}(hkl)|$ and the weighted one as $R_w := \{\sum w[F_{obs}(hkl) - F_{calc}(hkl)]^2\}/\sum w F_{obs}^2(hkl)$, where F_{obs} are the observed structure factors, F_{calc} the calculated ones, and the weights are derived from the counting statistics of the intensity measurements.

[21] J. E. Bertie and B. F. Francis, J. Chem. Phys. 77, 1 (1980).

[22] S. K. Sharma, H. K. Mao, and P. M. Bell, Phys. Rev. Lett. 44, 886 (1980).

[23] P. Pruzan, J. C. Chervin, and M. Gauthier, Europhys. Lett. 13, 81 (1990).